

1 **New insights into microbial community coalescence in the land-sea**  
2 **continuum**

3 Châtillon Elise<sup>a</sup>, Robert Duran<sup>a</sup>, François Rigal<sup>a</sup>, Christine Cagnon<sup>a</sup>, Aurélie Cébron<sup>b</sup>, Cristiana  
4 Cravo-Laureau<sup>a\*</sup>

5

6 <sup>a</sup> Université de Pau et des Pays de l'Adour, E2S UPPA, CNRS, IPREM, Pau, France

7 <sup>b</sup> Université de Lorraine, CNRS, LIEC, F-54000 Nancy, France

8 \*For correspondence: Postal address: Université de Pau e des Pays de l'Adour, Avenue de  
9 l'Université, Bâtiment IBEAS, BP 1155, 64013 Pau Cedex, France; Tel: +33 5 59 40 74 74 ; E-  
10 mail: cristiana.cravo-laureau@univ-pau.fr

11

12

13

14

15 **Abstract**

16 The land-sea continuum constitutes a mixing zone where soil microbial communities encounter,  
17 via runoff, those inhabiting marine coastal sediment resulting in community coalescence. Here,  
18 we propose an experimental approach, mimicking the land-sea continuum, to study the  
19 microbial community coalescence events in different situations, by 16S and 18S rRNA genes  
20 metabarcoding. The microbial community structure of sediment diverged with the soil inputs.  
21 For prokaryotes, phylogenetic enrichment and amplicon sequence variants (ASVs)  
22 replacements characterized the community changes in sediment receiving soil inputs. For fungi,  
23 despite phylogenetic enrichment was not observed, the fungal ASVs richness was maintained  
24 by soil inputs. Comparison of microbial communities revealed ASVs specific to sediment  
25 receiving soil inputs, and also ASVs shared with soil and/or runoff. Among these specific  
26 ASVs, four bacterial and one fungal ASVs were identified as indicators of coalescence. Our  
27 study provides evidences that coalescence involves the mixing of microorganisms and of the  
28 environment.

29

30 **Keywords**

31 microcosm, community coalescence, soil runoff, marine coastal sediment, indicator value,  
32 microbial indicator

### 33 **Introduction**

34 The land-sea continuum is a transition zone mixing terrestrial and marine coastal ecosystems,  
35 through diverse forms of connections, including direct inputs via rivers and flows from soil  
36 runoff. Inputs from the riverine network into marine environment have been shown to  
37 significantly change environmental parameters (e.g. nutrients and suspended particulate matter,  
38 salinity, pH) (Brannock et al., 2016; Jeffries et al., 2016) and also transport microorganisms  
39 (Halliday et al., 2014; Yakirevich et al., 2013), resulting in community coalescence. Thus,  
40 community coalescence corresponds not only to the blending of previously separated  
41 communities but also includes the mixing of their respective environments (Bandelj et al., 2012;  
42 Rillig et al., 2015). Studies of coalescence in marine environment have only considered the  
43 direct inputs via rivers in estuaries (Campbell and Kirchman, 2013; Crump et al., 2004, 1999;  
44 Fortunato and Crump, 2015; Mansour et al., 2018; Webster et al., 2015) while the inputs from  
45 soil runoff have been neglected within land-sea continuum. However, soil runoff, generated by  
46 rainfall, is widespread among coastal areas representing an important upload of terrigenous  
47 materials (plant debris, organic matter, mineral particles material and pollutants (Duran and  
48 Cravo-Laureau, 2016; Hoffman et al., 1984; Montgomery et al., 2000)) that reaches directly the  
49 sea without dilution in river. It is likely that microbial communities transported by these  
50 terrigenous materials coalesce with marine microbial communities, which remains to be  
51 demonstrated. The content of terrigenous materials depends on the vegetation cover that modify  
52 water flow (Nagase and Dunnett, 2012; Wenzel, 2009) and control the soil microbial  
53 communities. Therefore, it is worth considering the contribution of soil runoff to microbial  
54 community structure in marine coastal sediment. Additionally, land-based activities  
55 dramatically alter microbial processes (Fredston-Hermann et al., 2016) by disrupting microbial  
56 communities influenced by biotic and abiotic factors (Cravo-Laureau and Duran, 2014; Duran  
57 et al., 2015a; Pischedda et al., 2008), probably affected by terrigenous inputs from soil runoff.

58 Several studies have shown the influence of terrigenous inputs in the organization of microbial  
59 communities in water column (Crump et al., 2004, 1999; Logares et al., 2009; Paver et al.,  
60 2018; Wisnoski et al., 2020), but information is missing for marine sediment. Microbial  
61 communities play a pivotal role in the biogeochemical processes influencing ecosystem  
62 services (Falkowski et al., 2008; Graham et al., 2016; Nelson et al., 2016). For instance, the  
63 activity of microbial communities has been shown to be crucial in mitigating the effect of  
64 pollutants (Grizzetti et al., 2019), particularly hydrocarbons (HC) (McGenity et al., 2012) that  
65 accumulate in marine coastal sediment (Tolosa et al., 2004).

66 We hypothesize that soil runoff contributes to shape microbial communities inhabiting HC  
67 contaminated marine coastal sediment by the concomitant transfer of microorganisms and their  
68 environment (community coalescence), despite an asymmetric contribution due to dilution of  
69 soil runoff into marine habitat. In addition, the contribution of soil runoff depends on the soil  
70 vegetation cover and the presence of HC. In order to test this hypothesis, an experimental  
71 ecology approach was set up to mimic soil runoff within land-sea continuum in microcosm.  
72 This experiment was specifically designed to consider the effect of plant and HC influencing  
73 potentially the runoff, and in turn modulate the coalescence events.

74 Changes in marine sediment microbial community across experimental conditions were  
75 revealed by quantifying shifts in community diversity and composition for both prokaryotic and  
76 fungal assemblages. Microbial communities were characterized by Illumina sequencing of the  
77 16S and 18S rRNA genes allowing their comparison in the different situations.

## 78 **Material and Methods**

### 79 **Soil and sediment samples**

80 Soil (10 kg) and sediment (2 kg) were collected in the same geographical area, in southeast of  
81 France, in October 2017. Soil came from the surroundings of the Berre Pond (43°29'6.9"N

82 5°11'18.53"E, France) and sediment from the Canal Vieil Cove (43°23'20.3"N 4°59'31.8"E,  
83 France). Both sites are close to petroleum refinery and constitute a model of a realistic HC  
84 contaminated land-sea continuum. Prior to microcosms setup, soil and sediment were sieved to  
85 <4 mm and <1 mm, respectively, to homogenize, remove coarse gravels, plant debris and  
86 macroorganisms. The whole soil sample and a part of the sediment sample were air dried under  
87 a cupboard. The rest of the sediment was stored at 4 °C in a 5 L bottle completely covered with  
88 *in situ* seawater and with continuous aeration through an aquarium pump. Soil and sediment  
89 characteristics were determined on dry samples at the Laboratoire d'Analyses des Sols - LAS  
90 (INRAe, Arras, France). The soil had a loamy and sediment a sandy texture (23.4% and 4.7%  
91 clay, 38.5% and 4.5% silt, 38.1% and 90.8% sand, for soil and sediment, respectively). Both  
92 soil and sediment showed basic pH (8.4 and 9.1 for soil and sediment, respectively). The C/N  
93 ratio was about 30.0 and 46.6 for soil and sediment, respectively. The organic carbon content  
94 and the total nitrogen were higher in soil than in sediment (35.4 and 18.6 g C/kg, 1.2 and 0.4 g  
95 N/kg). The cation-exchange capacity estimated by cobaltihexamine method is higher in soil  
96 than in sediment (15.9 and 1.4 cmol+/kg).

### 97 **Microcosms Setup**

98 An original microcosm system was set up under controlled conditions at the laboratory (

99 Figure 1). The experimental design was drawn with the aim to test the hypothesis that the soil  
100 runoff influences the structure and the composition of microbial communities in downstream  
101 sediment depending on the presence of plants and/or on HC. For this purpose, two kinds of  
102 microcosms were set up (

103 Figure *IA*): the land-sea continuum microcosms (R) that simulated the soil runoff to marine  
104 coastal sediment connecting soil and sediment compartments; and the control microcosms (NR)  
105 without runoff of soil consisting of single sediment compartment. Briefly, the microcosms were  
106 composed of glass devices (1 L beaker equipped with an inlet and outlet) containing the  
107 equivalent of 100 g of dry sediment covered with seawater (Salt Instant Ocean, Aquarium  
108 systems, concentration 35 g/L). For the land-sea continuum microcosm, these devices were  
109 connected through Teflon pipes to stainless steel devices containing 600 g of dry soil moistened  
110 at 60% water holding capacity. Different conditions were applied in triplicate combining the  
111 presence of plant (P) or not (NP) in soil with the spiking of deuterated HC (C) or not (NC) in  
112 soil and sediment (

113 Figure *IB* and C). Thus, six different experimental conditions were compared. In the HC spiked  
114 conditions, soil and sediment (1/10 of the soil and sediment as dry weight) received a mix 1:1  
115 (W:W) of deuterated n-hexadecane (D34, 98%, Cambridge Isotope Laboratories, Inc, USA)  
116 and phenanthrene (D10, 98%, Euriso-top, France), dissolved in hexane solvent. A stock  
117 solution was prepared in order to add each HC at a concentration of 1000 mg/kg dry soil or  
118 sediment. For the unspiked conditions, the same volume of hexane was added alone without  
119 addition of HC stock solution. After total solvent evaporation, 9:10 of crude soil and sediment  
120 were mixed with spiked fractions to have a contamination at 100 mg/kg. Soils were watered to  
121 reach 60% of their water holding capacity. *Catapodium marinum*, a grass identified *in situ*, was  
122 sown in soil with 25 seeds (seed bank of the Muséum National d'Histoire Naturelle, Paris,  
123 France) per microcosm. For the sediment compartment, 200 mL of seawater was added on the  
124 top of the sediment. After an aging period of 4 days at 4 °C, allowing the sorption of the HC  
125 into soil and sediment matrices, microcosms were installed in a phytotronic chamber with  
126 controlled conditions (22 °C/18 °C day/night, 80% relative humidity, c.a. 250  $\mu\text{mol photons}$   
127  $\text{m}^{-2} \text{s}^{-1}$ , 16 h photoperiod). Microcosms were incubated for 39 days, the estimated time  
128 necessary for plant growth and HC degradation (Ben Said et al., 2015; Bourceret et al., 2017;  
129 Duran et al., 2015b). Soil compartments were watered five consecutive days per week by means  
130 of a syringe dispensing 73 mL mineral water (Volvic®) to mimic rainfall and produce soil  
131 runoff and in turn terrigenous inputs. After seed germination, 16 plants were kept per device.  
132 Both in land-sea continuum and in control microcosms, peristaltic pumps helped to simulate a  
133 12 h tidal cycle. In this way, the seawater was renewed twice a day maintaining sediment  
134 covered by 3 cm of seawater during the low tide ensuring conditions close to those prevailing  
135 in natural environment.



## 136 **Sampling**

137 Samples of the different compartments (soil, runoff, sediment) and of seawater were collected  
138 at different times: at the beginning, at the end, and during the incubation for subsequent  
139 biomolecular analysis. Soil and sediment samples (ca. 10-12 g) were collected in triplicates at  
140 the beginning and end of the experiment (t<sub>0</sub> and t<sub>f</sub>, respectively) for the DNA extraction. Soil  
141 samples were collected using a little stainless steel corer (diameter: 14 mm; height: 40 mm, 31)  
142 and sediment samples using a spatula. At t<sub>0</sub>, three soil samples (each being the mixture of 3  
143 cores) were collected from two additional soil devices, one with HC spiking and one without  
144 HC spiking, so as not to alter soil structure or disturb plant germination in devices that continued  
145 the incubation. Three sediment samples (each being the mix of 3 subsamples) were collected  
146 from the sediment batch prepared for sediment devices with HC spiking (NPC, PC, NRC  
147 conditions) and from the one prepared for sediment devices without HC spiking (NPNC, PNC,  
148 NRNC conditions). Runoff samples were collected from each land-sea microcosms, by mixing  
149 runoff from three consecutive days, at t<sub>1</sub> (days 16, 17 and 18 of incubation) and at t<sub>2</sub> (days 31,  
150 32 and 33 of incubation). Runoff samples (45 mL) and 45 mL of Volvic water (rainwater) as  
151 control were filtered at 0.22 µm (Millex). At t<sub>f</sub> (after 39 days of incubation), *Catapodium*  
152 *marinum* were cut at the collar before soil sampling. Soil samples were collected in triplicate  
153 from each land-sea continuum microcosm using a template (three notches per row and three per  
154 column) as a guide for the corer. The cores from the same column were mixed and formed one  
155 sample. Sediment samples were collected from each microcosm after mixing of sediment. Soil,  
156 runoff (filters) and sediment samples were stored at -80°C.

## 157 **DNA extraction and rRNA gene sequencing**

158 DNA was extracted from 250 mg of soil or sediment sample and from the filter of runoffs using  
159 the PowerSoil DNA Isolation Kit (MoBio Laboratories) according to the manufacturer's  
160 recommendations. PCR amplification of the V4-V5 hypervariable region of the 16S rRNA gene

161 was performed using the Archaea/Bacteria primers 515F (5'-GTG-YCA-GCM-GCC-GCG-  
162 GTA-3') and 928R (5'-CCC-CGY-CAA-TTC-MTT-TRA-GT-3') (Parada et al., 2016; Wang  
163 and Qian, 2009). Likewise, 18S rRNA gene was also amplified using the eukaryotic primers  
164 FF390 (5'-CGA-TAA-CGA-ACG-AGA-CCT-3') and FR1 (5'-AIC-CAT-TCA-ATC-GGT-  
165 AIT-3') targeting the V7-V8 region (Chemidlin Prévost-Bouré et al., 2011; Vainio and Hantula,  
166 2000). The reverse and forward primers included Illumina adapters. Before amplification, the  
167 concentration of DNA was determined with a Quant-It kit in microplate in order to normalize  
168 the following amplification. Amplifications were performed in triplicate in a total volume of 25  
169  $\mu$ L reaction mixture containing 0.8  $\mu$ M or 0.4  $\mu$ M of each primer for Archaea/Bacteria and  
170 Eukaryote respectively, 2 ng or 4 ng of DNA for Archaea/Bacteria and Eukaryote respectively,  
171 12.5  $\mu$ L of AmpliTaq Gold 360 Master Mix (Applied Biosystems). The final volume was  
172 adjusted with distilled water. Cycling conditions were: an initial denaturation step at 95 °C for  
173 10 minutes, followed by 35 cycles with denaturation step at 95 °C for 30 s, hybridization step  
174 at 60 °C for 30 s or at 50 °C for 45 s (for Archaea/Bacteria primers and Fungi primers,  
175 respectively), and elongation step at 72 °C for 40 s or 30 s (for Archaea/Bacteria primers and  
176 Fungi primers, respectively), after which a final elongation step at 72 °C for 10 minutes was  
177 performed. The 2 $\times$ 250 paired-end sequencing was carried out at the Genotoul platform  
178 (Toulouse, France) with Illumina-MiSeq. Raw sequence data for the amplicon data were  
179 deposited in the Sequence Read Archive (SRA) of the National Center for Biotechnology  
180 Information (NCBI) and is available under the assigned Bioproject PRJNA803214  
181 (<https://dataview.ncbi.nlm.nih.gov/object/PRJNA803214>).

182

### 183 **Sequence processing and ASV delimitation**

184 The open source software Qiime2 (Bolyen et al., 2019) was used for 16S and 18S rRNA gene  
185 read analysis. Sequencing resulted in 3 735 622 and 3 716 691 raw reads for prokaryotic and

186 eukaryotic datasets, respectively (Table S1). The rarefaction curves (Fig. S1) showed that most  
187 of the diversity was captured during the sequencing. The two datasets were first demultiplexed  
188 and dada2 (Callahan et al., 2016) was used to control reads quality and infer amplicon sequence  
189 variants (ASVs) (Callahan et al., 2017). Default settings were used except that reverse reads  
190 were truncated to 230 base pairs before merging. This denoising step resulted in 6 988 and 2  
191 488 ASVs for prokaryotic and eukaryotic datasets, respectively (Table S1). The taxonomy was  
192 assigned to the ASVs with a fixed sequence similarity threshold of 97 % using the SILVA  
193 database release 132 for 16S and 18S rRNA gene sequences (Quast et al., 2013). Then, ASVs  
194 assigned to mitochondria and chloroplasts and ASVs unassigned at the domain level were  
195 further removed from the datasets resulting in 6 748 prokaryotic ASVs (Table S1). For  
196 Eukaryotes, only ASVs affiliated to Fungi were retained resulting in 705 fungal ASVs (Table  
197 S1). Phylogenetic trees were constructed using FastTree (Price et al., 2010) in the Qiime2  
198 phylogeny plugin. The phylogenetic tree was made ultrametric (i.e. all tips equidistant from the  
199 root) for the following analyses using the “chronos” function in the R package ape (Paradis and  
200 Schliep, 2019) with branch lengths representing relative time (root at 1 and tips at 0). The  
201 number of reads for each sample was rarefied to the same number corresponding to the  
202 minimum read number per sample (7 578 sequences) for prokaryotic dataset (Fig. S1). The  
203 same procedure was carried out for the fungal dataset (i.e. with a minimum read number per  
204 sample of 1 027 sequences), after having removed two samples with too low read number  
205 (Runoff PC t2-3 and SedR PNC tf-1) (Fig. S1). The rarefaction was performed with R software  
206 using phyloseq package (McMurdie and Holmes, 2013). These thresholds are trade-offs  
207 reflecting the need to maximize sampling effort while preserving most of the samples according  
208 to the rarefaction curves (Fig. S1). The prokaryotic dataset encompassed 66 samples whereas  
209 fungal datasets 64 samples. The following statistical analyses were implemented within the R  
210 programming environment (R Core Team, 2021).

211 Metabolic and ecological functions of prokaryotic and fungal communities were predicted  
212 using FAPROTAX (Louca et al., 2016) and FUNGuild (Nguyen et al., 2016) respectively.

### 213 **Alpha and beta-diversity of the core microbial communities**

214 Prior to the diversity analyses, the ASVs were partitioned into core (abundant and widely  
215 distributed) and satellite (low abundant and limited distribution) groups. It has been shown that  
216 the interpretation of biodiversity patterns reacting to environmental change was improved by  
217 combining abundance and occurrence of taxa (Jeanbille et al., 2016; Lindh et al., 2017). The  
218 core community has been demonstrated to be high sensitive to environmental changes and the  
219 presence of contaminants while the distribution of the satellite group has been shown to be  
220 mostly random (Jeanbille et al., 2016). The core and satellite groups were identified as follow:  
221 first, the correlation between the relative abundance and the occurrence of each ASV was  
222 calculated throughout the dataset. Then, the index of dispersion of each ASV was calculated as  
223 the ratio of the variance to the mean abundance multiplied by the occurrence (Jeanbille et al.,  
224 2016). The ASVs were partitioned into core (abundant and widely distributed) and satellite (low  
225 abundant and limited distribution) groups (Hanski, 1982; Hu et al., 2017; Magurran and  
226 Henderson, 2003; Ulrich and Zalewski, 2006). The ASVs were considered as core if their index  
227 of dispersion deviated from a random Poisson distribution fall outside the 95% confidence  
228 interval of the  $\chi^2$  distribution (Jeanbille et al., 2016; Unterseher et al., 2011; van der Gast et al.,  
229 2011). In order to characterize the core and the satellite groups according to the level of the  
230 habitat specialization, the Levins' niche breadth index (Levins, 1968) was calculated using  
231 levins.Bn function in the R package MicroNiche (Finn et al., 2020). A Wilcoxon rank sum test  
232 was performed to compared the niche breadth index of the core and the satellite groups.  
233 Therefore, the subsequent analyses were focused on the core group. Alpha and beta-diversity  
234 were quantified at both taxonomic and phylogenetic level. For alpha-diversity, the indices ASV  
235 richness and Inverse Simpson index (i.e. the Hill number of order 2,  ${}^2D$ ) were selected as well

236 as their phylogenetic equivalents namely the Faith's phylogenetic diversity index (Faith's PD)  
237 and the Hill2 phylogenetic diversity index ( ${}^2$ PD) respectively. In order to identify changes in  
238 alpha-diversity among conditions, two-way analyses of variance (ANOVA) were performed  
239 using two factors, HC spiking (NC, C), and a factor grouping the other conditions (t0, NP tf  
240 and P tf for soil; t0, NR tf, R NP tf and R P tf for sediment), and their two-ways interactions.  
241 When factors were significant, post hoc tests (Tukey's HSD test) were performed to identify  
242 conditions that were significantly different from each other. Beta-diversity between all pairs of  
243 samples were quantified using the weighted Jaccard dissimilarity index for ASV and weighted  
244 UniFrac for phylogenetic (branches) beta-diversity (Lozupone and Knight, 2005). Prior to the  
245 analyses, the abundances were square root transformed. Following Cardoso et al. (2015), the  
246 total beta-diversity ( $\beta_{tot}$ ) for both Jaccard and UniFrac was partitioned into its replacement  
247 ( $\beta_{repl}$ ) and richness difference ( $\beta_{rich}$ ) components in order to decipher the different process  
248 underlying the change in community assembly;  $\beta_{repl}$  reflects true turn-over and  $\beta_{rich}$  quantifies  
249 the loss and gain of ASV between communities. Beta partitioning was implemented with R  
250 package BAT (Cardoso et al., 2015). Patterns of beta-diversity were visualized using a non-  
251 metric multidimensional scaling (NMDS). PerMANOVA (permutational multivariate analysis  
252 of variance) based on 9 999 permutations were implemented using adonis2 function from vegan  
253 R package (Oksanen et al., 2013) to test the effect of the different conditions in each  
254 compartment (soil, runoff, sediment). Post-hoc tests were conducted using pairwise  
255 comparisons to identify conditions that were significantly different from each other.

### 256 **Venn diagram, microbial source tracking and indicator species analyses**

257 The web-based tool InteractiVenn (Heberle et al., 2015) was used to analyse and visualize the  
258 shared presence of prokaryotic and fungal ASVs among soil, runoff and sediment according to  
259 runoff treatment.

260 An indicator analysis was performed to identify ASVs that were associated with a specific  
261 condition or a combination of conditions using the Dufrene and Legendre indicator value (ie.  
262 IndVal) (Dufrière and Legendre, 1997) in the R package indicpecies (Caceres and Legendre,  
263 2009). IndVal index quantifies the strength of the association by combining information on  
264 ecological specificity and fidelity for each ASV. IndVal value range from 0 (no association) to  
265 1 (perfect association). Significance of IndVal values were assessed using permutation tests (N  
266 = 9 999) under the null hypothesis of no association.

267 Microbial source tracking analysis was conducted using SourceTracker2 (version 2.0.1;  
268 Knights et al., 2011) to identify the contribution of soil and runoff microbial communities as  
269 source for those of sediment with runoff.

## 270 **Results and discussion**

### 271 **Partitioning the microbial community into core and satellite groups**

272 The experiment was specifically designed to investigate the microbial coalescence in a land-  
273 sea continuum i.e. the contribution of soil and soil microbial community inputs (via soil runoff)  
274 in shaping the marine coastal sediment microbial community. For this purpose, the microbial  
275 community composition of the different compartments (soil, runoff, and sediment), collected  
276 at the beginning and at the end of the experimental incubation, was determined by high  
277 throughput sequencing. For the prokaryotic and eukaryotic communities, 3 735 622 and 3 716  
278 691 raw reads were respectively obtained (Table S1). The observed richness rarefaction curves  
279 (Fig. S2) reached a plateau suggesting the sampling depth was sufficient to capture the diversity.  
280 After trimming and rarefaction, 7 578 and 1 027 sequences were respectively affiliated to 6 064  
281 prokaryotic and 638 fungal ASVs (Table S1). The ASVs abundance distribution showed that  
282 the microbial communities were distributed into core and satellite ASVs groups, the mean  
283 ASVs abundance being positively linked to the occurrence (Fig. S2A), as already evidenced

284 (Hu et al., 2017; Jeanbille et al., 2016; Lindh et al., 2017). The core and satellite ASVs were  
285 identified by examining the relationship between the index of dispersion and occurrence of each  
286 ASV (Fig. S2B). Most of the microbial ASVs (4 462 prokaryotic and 465 fungal ASVs; Table  
287 S1) fitted a random distribution (Poisson model) defining the satellite ASVs. In contrast, 1 602  
288 prokaryotic and 173 fungal ASVs formed the non-randomly distributed core ASVs (Table S1).  
289 This core microbial community contained less than 30 % of the total ASVs, accounting for  
290 more than 80 % of the total reads. The core microbial community had a significantly wider  
291 (Wilcoxon test:  $W = 68\,363$   $p < 0.001$ , Fig. S3) niche breath than the satellite community. This  
292 feature suggests that the microbial core community includes generalists able to use widespread  
293 resources (Brown, 1984). In addition, studies showed that the core microbial community brings  
294 information reporting the effect of the environmental factors (Jeanbille et al., 2016; Magurran  
295 and Henderson, 2003; Ulrich and Zalewski, 2006) which allow us to focus on the core microbial  
296 community in order to characterize the microbial communities inhabiting mixing zone  
297 influenced by soil runoff.

### 298 **Diversity of the core microbial community**

299 Using ASV and phylogenetic alpha-diversity indices, the effects of plant, HC spiking and soil  
300 runoff were investigated in the core microbial communities inhabiting soil and sediment (Fig.  
301 2). Prokaryotic and fungal soil richness (R) and the inverse Simpson ( $^2D$ ) indices remained  
302 stable along the course of the experiment while the Faith's PD increased (ANOVA 16S:  $F =$   
303  $5.07$ ,  $p < 0.05$ ; ANOVA 18 S:  $F = 12.65$ ,  $p < 0.05$ ), irrespective of the presence of plants (NP,  
304 P), with a significant additional increase (Tukey's test: Soil C t0 – Soil C tf,  $p < 0.05$ ) in HC  
305 spiking samples (Fig. 2A and B). It was surprising to observe that the presence of plants was  
306 not affecting the soil microbial diversity although plant roots exudates have been shown to  
307 provide nutrients (Van Hecke et al., 2005) and promote the development of microorganisms  
308 carrying HC degrading genes (Cébron et al., 2011; Toyama et al., 2011). Regarding the

309 sediment microbial diversity, similar trends were observed for the prokaryotic communities  
310 with a significant temporal increase of <sup>2</sup>PD (ANOVA 16S: F = 6.79, p < 0.05) irrespective of  
311 the condition, while the fungal diversity was not affected (Fig. 2C and D). Sediment receiving  
312 terrigenous inputs and with HC spiking had the highest prokaryotic <sup>2</sup>PD, showing increased  
313 phylogenetic enrichment due to both runoff and HC spiking (Tukey's test: Sed t0 - SedR C tf,  
314 p < 0.05; Fig. 2C). Such HC effect on prokaryotic community was consistent with previous  
315 studies showing i/ modification of microbial communities after petroleum addition (Bordenave  
316 et al., 2004; Chronopoulou et al., 2013; Stauffert et al., 2014), and ii/ an increase of microbial  
317 diversity, especially in historically HC contaminated sediments (Duran et al., 2015b; Jeanbille  
318 et al., 2016; Paissé et al., 2008). The diversity increase was explained by the legacy effect of  
319 previously exposed microbial communities to pollutants (Ben Salem et al., 2019) and  
320 environmental disturbances (Jurburg et al., 2017; Nunes et al., 2018). In our study, the observed  
321 increase of phylogenetic enrichment due to both runoff and HC spiking suggested that runoff  
322 transferred microorganisms from soil to sediment, which probably resulted in microbial  
323 community coalescence as reported for river sediment (Mansour et al., 2018), relating  
324 modifications in the microbial community composition.

### 325 **Microbial composition within the land-sea continuum compartments**

326 In order to have an overview of the composition of the microbial community within the land-  
327 sea continuum, the relative abundance of the phyla in the different compartments (soil, runoff,  
328 sediment) was examined. Overall, most ASVs were affiliated to twelve bacterial and eight  
329 fungal phyla (Fig. 3). ASVs affiliated to Archaea belonged to Nanoarchaeota and  
330 Thaumarchaeota phyla with relative abundance less than 1% of prokaryotes. Proteobacteria  
331 dominated the prokaryotic communities (21±7%, 60±14% and 60±22% in soil, runoff and  
332 sediment, respectively; Fig. 3A and Table S2) while the Ascomycota dominated the fungal  
333 communities, except in runoff in which most fungi were unassigned (65±7% and 80±17% of



334 Ascomycota in soil and sediment, respectively, and  $47\pm 12\%$  of unassigned fungi in runoff; Fig.  
335 3B and Table S3). As expected, the compartments along the continuum (soil, runoff, and  
336 sediment) exhibited different microbial community composition. Soil was characterized by the  
337 presence of Acidobacteria, Actinobacteria and Betaproteobacteria (23 %, 21 % and 8 %,  
338 respectively). In runoff and sediment, Proteobacteria (60%) and Bacteroidetes (~20%)  
339 predominated (Fig. 3A). As in soil, the runoff was dominated by Betaproteobacteria (23%),  
340 whereas in sediment Gammaproteobacteria and Deltaproteobacteria (32 and 19%, respectively)  
341 prevailed, which is in accordance with previous studies showing that Gammaproteobacteria and  
342 Deltaproteobacteria are abundant in HC contaminated coastal sediments (Acosta-González and  
343 Marqués, 2016; Stauffert et al., 2015). Regarding the fungal community (Fig. 3B), Ascomycota  
344 was the dominant phylum in soil and sediment (65 and 80 %, respectively), followed by  
345 Basidiomycota (15 %) in soil and Chytridiomycota (14 %) in sediment, which is consistent with  
346 the fact that these phyla have been found in diverse ecosystems (Amend et al., 2019; Bahram  
347 et al., 2018; Comeau et al., 2016; Kohlmeyer and Kohlmeyer, 1979). In runoff, most fungi were  
348 unassigned (almost 50 %), showing that a large part of soil fungal diversity transported by soil  
349 runoff remains unknown and corresponds to the low abundant soil fungal taxa. Thus, simulated  
350 soil runoff represents a way to reveal undescribed soil fungal diversity. The difference between  
351 compartments was also observed at the functional level using predictive FAPROTAX (Figure  
352 S4) and FUNGuild (Figure S5) tools. A total of 478 functional assignments for 1602  
353 prokaryotic ASVs were obtained, revealing that sediment is characterized by the presence of  
354 metabolisms involved in the sulfur cycle. Only 13.9% of the fungal ASVs (24 out of the 173)  
355 were assigned to guilds, mostly represented in soil by plant parasite-saprotroph fungi, runoff  
356 dominated by endophyte- saprotroph fungi while the sediment was characterized by unassigned  
357 guilds highlighting the lack of data about marine fungi. The use of more powerful techniques  
358 as metagenomic or functional DNA arrays is required to reveal similarities and differences

359 between the three compartments and under the different conditions. Nevertheless, overall,  
360 distinct microbial communities were identified in each compartment consistent with the alpha-  
361 diversity analysis. Thus, the experimental design allows the study of coalescence by mixing  
362 different microbial communities.

### 363 **Comparison of microbial communities**

364 In order to characterize the coalescence, further comparisons between microbial communities  
365 were performed, particularly the detection of shift in microbial community composition (ASV  
366 and phylogenetic) due to terrigenous inputs using betadiversity partitioning. Overall, the  
367 comparison of the microbial community composition between samples by NMDS based on the  
368 weighted UniFrac metric showed three clusters corresponding to the three compartments (soil,  
369 runoff and sediment) for both prokaryotes and fungi (Figure 4A and B respectively). Significant  
370 differences in the ASV and phylogenetic microbial composition between the compartments  
371 (Figure 4) were observed (ASV and phylogenetic  $\beta_{tot}$ , PerMANOVAs: all p-values < 0.001  
372 Table S2). Such observations highlighted that each compartment contained specific ASVs and  
373 lineages, in accordance with the presence of habitat filtering mechanisms (Lozupone and  
374 Knight, 2007). The fact that runoff microbial communities (prokaryotic and fungal) were  
375 distinct from those of soil (ASV and phylogenetic  $\beta_{tot}$ , Post-hoc tests: all p-values < 0.001,  
376 Table S2, Figure 4) showed that the microbial component of the terrigenous inputs represented  
377 only part of the soil diversity. This result suggests that only a subset of soil microorganisms and  
378 soil aggregates was able to flow in runoff, which depends on the microbial lifestyle and the soil  
379 properties allowing more or less their detachment from the matrix (Holmsgaard et al., 2011).  
380 In both soil and runoff (Fig. 4), the microbial ASV composition changed with time and with  
381 the HC spiking (ASV  $\beta_{tot}$ , PerMANOVAs: time: all p-values < 0.001, HC spiking: all p-values  
382 < 0.05, Tables S3, S4), irrespective of the presence of plant (ASV  $\beta_{tot}$ , PerMANOVAs: all p-  
383 value > 0.05, Tables S3, S4). In sediment, the prokaryotic community behaviour was different

384 to that of the fungal community. Two clusters separated the prokaryotic community according  
385 to time (Figure 4A) while the fungal community was separated into two clusters according to  
386 runoff treatment (Figure 4B). For prokaryotes, the replacement of ASVs explained the  
387 differences between clusters observed at the beginning and at the end of the experiment (ASV  
388  $\beta$ repl, PerMANOVA and Post-hoc tests: all p-values<0.001, Table S5). The effect of the  
389 terrigenous inputs was not observed, despite that alpha diversity showed an enrichment,  
390 probably hidden by the effect of time. For fungi, the clusters contained different ASVs  
391 corresponding to lineage richness modifications, explained by the loss of richness in sediment  
392 without terrigenous inputs (SedNR tf) (phylogenetic  $\beta$ rich, PerMANOVA and Post-hoc tests:  
393 all p-values < 0.01, Table S5) reflecting that the compartments were not connected. In contrast,  
394 the fungal phylogenetic richness was maintained by terrigenous inputs, suggesting that the lack  
395 of runoff affect the fungal community. It is likely that the terrigenous inputs simulated in our  
396 experiment mimicking *in situ* coalescent event explained the resilience of the fungal community  
397 in sediment observed only with runoff.

398 The microbial communities from the three compartments were further compared by Venn  
399 diagrams in order to identify the shared and specific microbial ASVs (Figure 5). No ASVs  
400 shared by the compartments was identified for the prokaryotic communities (Figure 5A), while  
401 five shared ASVs were identified for the fungal communities (Figure 5 B). This result  
402 corroborates the structuration of the microbial communities in different compartments. Soil and  
403 runoff shared the highest number of prokaryotic and fungal ASVs (336 ASVs and 27 ASVs  
404 respectively; Figure 5A and B), as expected since beta-diversity analysis showed that runoff is  
405 a subset of soil. Interestingly, runoff was mostly constituted of specific prokaryotic ASVs (408  
406 ASVs, Figure 5A), supporting the hypothesis that a large part of soil microbial diversity  
407 transported by soil runoff corresponded to the low abundant soil taxa. The sediment receiving  
408 terrigenous inputs exhibited 48 prokaryotic (Figure 5A) and three fungal specific ASVs (Figure

409 5B), which indicates that these ASVs were below the detection threshold in both soil and  
410 sediment at the beginning of the experiment (Soil t0 and Sed t0), they emerged in the sediment  
411 receiving terrigenous inputs during the experiment (SedR tf). We hypothesize that these specific  
412 ASVs correspond to i/ sediment taxa benefiting from the terrigenous inputs, and ii/ soil taxa  
413 transferred to sediment. It is likely that terrigenous inputs favoured the development of specific  
414 ASVs because sediment without terrigenous inputs (Sed NR tf) exhibited only eight specific  
415 ASVs. These results are in accordance with previous studies showing the loss of specialists and  
416 the emergence of taxa during coalescence event (Logares et al., 2009; Paver et al., 2018; Rocca  
417 et al., 2020; Wisnoski et al., 2020). Focusing on the ASVs shared by soil, runoff and sediment  
418 receiving terrigenous inputs, 4 prokaryotic (Figure 5A) and 13 fungal (Figure 5B) ASVs were  
419 identified, indicating the potential transfer of ASVs within the soil and marine coastal sediment  
420 continuum. Consistently, the microbial source tracking analysis conducted with  
421 SourceTracker2 identified terrigenous inputs as minor sources for fungal communities in  
422 sediment at the end of the experiment, irrespective of the runoff treatment (soil or runoff  
423 estimated fungal contributions ranged between 0.01% and 3.18% except for two sediment  
424 without runoff samples for which these contributions were null; Table S8). Soil and runoff  
425 fungal contributions were especially increased in sediment with runoff (Wilcoxon tests:  
426  $W=57$ ,  $p\text{-value}<0.01$  for soil;  $W=66$ ,  $p\text{-value}<0.001$  for runoff) compared to sediment without  
427 runoff. In contrast, soil and runoff were not reported by the analysis as sources for prokaryotic  
428 communities in sediment at the end of the experiment except for three samples out of 18  
429 (exclusively sediment with runoff samples) for which soil or runoff prokaryotic contributions  
430 were less than 1% (Table S8). The low number of shared microbial ASVs and the low  
431 contributions of soil and runoff as source show that many microbial taxa present in runoff did  
432 not persist in the sediment they entered. They probably do not have the capacity to deal with  
433 the new conditions (salinity, pH, oxygen) and niche competition, prevalent in sediment. They

434 may have been diluted or washed away during the renewal of seawater. Among the 4 shared  
435 prokaryotic ASVs, two were affiliated to Gammaproteobacteria (*Legionella* and *Massilia*), one  
436 to Bacteroidia (*Terrimonas*) and one to Actinobacteria (*Williamsia*). The fungal ASVs were  
437 affiliated to Dikarya (Ascomycota), LKM15 group, Chytridiomycota (Chytridiomycetes),  
438 Mucoromycota (Mucoromycotina, Mucorales) and Cryptomycota. It is likely that these  
439 transferred microorganisms characterized the microbial community coalescence event. The  
440 distribution of the prokaryotic transferred ASVs in the land-sea continuum showed that  
441 *Legionella* (ASV1184) and *Massilia* (ASV1436) were found at low abundance in soils,  
442 enriched in runoff, and detected only in HC spiked sediment receiving terrigenous inputs from  
443 unplanted soil (SedR NPC tf; Figure 5C). Microorganisms affiliated to these taxa are found in  
444 various ecosystems (Engleberg, 2009; Ofek et al., 2012), including HC contaminated  
445 environments (Gu et al., 2016), and characterized by motile capacity (Engleberg, 2009; Ofek et  
446 al., 2012) explaining their enrichment in the runoff. *Terrimonas* (ASV4242) was present in soil  
447 compartment in the different microcosms and poorly represented in runoff and sediment  
448 receiving terrigenous inputs, which is consistent with the fact that it is a non-motile soil  
449 microorganism (Board, 2015). *Williamsia* (ASV6220) was not specific to a compartment  
450 (Figure 5C). Environmental members from this genus have been isolated from oil-contaminated  
451 soil and deep-sea sediments (Pathom-Aree et al., 2006; Stach et al., 2004; Yassin et al., 2007).

452 Among the 14 fungal transferred ASVs, four ASVs were the most abundant, showing a  
453 particular distribution (Figure 5D). Noteworthy, Cryptomycota (ASV234) and LKM15 (ASV4  
454 and ASV15) were enriched in runoff. Recent studies revealed the importance of these early  
455 diverging lineages in freshwater lakes and marine environments (Rojas-Jimenez et al., 2017).  
456 In particular, they produce motile aquatic spores (Money, 2016) and are able to parasitize the  
457 phytoplankton, which are advantages for inhabiting aquatic ecosystems (Rojas-Jimenez et al.,  
458 2017), supporting their enrichment in runoff. *Hypocreales* (ASV525) was present in soil, runoff

459 and sediment receiving terrigenous inputs, irrespective of the condition (Figure 5D).  
460 *Hypocreales* are common in terrestrial and marine (seawater and sediment) environments  
461 (Jones et al., 2015; Torres and White, 2009). Their particle associated lifestyle (Pang et al.,  
462 2019; Torres and White, 2009) may explain their persistence along the land-sea continuum.  
463 These results, based on the presence/absence of ASVs, indicate that sediment with runoff  
464 owned specific microbial population, either coming from or favoured by terrigenous inputs,  
465 supporting the microbial community coalescence between compartments.

#### 466 **Identification of community coalescence microbial indicators**

467 In order to deeper characterize the ASVs participating in the coalescence, the identification of  
468 indicators, based on ASV relative abundances, was performed in sediment receiving terrigenous  
469 inputs by runoff (SedR). The ASV indicator value analysis, comparing the distribution of  
470 microbial population in the sediment compartment under the different conditions, revealed three  
471 bacterial ASVs and one fungal ASV significantly associated ( $p$  value $<0.05$ ) to the sediment  
472 with runoff (SedR) (Table 1). Interestingly, the distribution of these bacterial and fungal ASV  
473 SedR indicators among all compartments showed that the three bacterial ASVs were associated  
474 with sediment, in particular at the end of the experiment (Sed tf) while the fungal ASV was  
475 associated with soil (Table 1), which was in accordance with the Venn analysis (Figure 5).  
476 These results further support that specific bacterial ASVs correspond to sediment taxa  
477 benefiting from the terrigenous inputs while the specific fungal ASV corresponds to soil taxa  
478 transferred to sediment, showing the biotic and abiotic transfers resulting in community  
479 coalescence. Although the community coalescence, involving biotic and abiotic transfers,  
480 showed by Rocca et al. (2020) in laboratory experiment, have been suspected in field  
481 investigations (Crump et al., 2004, 1999; Logares et al., 2009; Paver et al., 2018; Wisnoski et  
482 al., 2020), our experimental ecology approach provide a set of evidences that coalescence in  
483 land-sea continuum involves the mixing of both microorganisms and the environment.

484 **Conclusion**

485 Our experimental ecology approach mimicking the land-sea continuum revealed that soil runoff  
486 modified the microbial communities inhabiting HC contaminated marine coastal sediment. The  
487 comparison of microbial communities, based on high throughput sequencing, identified  
488 bacteria and fungi taxa specific to sediment receiving soil inputs via soil runoff. The in-depth  
489 analysis of these specific taxa distinguished two ways of community coalescence: i/ the transfer  
490 of soil microorganisms, and ii/ the development of sediment taxa favoured by soil inputs. The  
491 community coalescence may result in the modification of the ecological niches constraining the  
492 functional organization of microbial communities and their role in biogeochemical cycles. In  
493 order to obtain a comprehensive view of microbial communities in coastal marine sediment, we  
494 advocate considering coalescence events, particularly for the monitoring and management of  
495 HC contaminated areas.

496 **Acknowledgments**

497 We thank the TOTEM project team for discussions and technical assistance. The seed bank of  
498 the Muséum National d'Histoire Naturelle de Paris - DGD MJZ is acknowledged for providing  
499 seeds of *Catapodium marinum*. Authors thank Manon Runza and Pauline Latour for setting up  
500 the experimental devices, and members of the Experimental phytotronic platform of Lorraine  
501 (PEPLor) at the Université de Lorraine (Site FST, Vandoeuvre-les-Nancy) for technical  
502 assistance and access to plant growth facilities.

503 **Funding**

504 This work was supported by the French national programme EC2CO-LEFE (TOTEM project).  
505 EC was supported by E2S-CCLLO grant.

506

507 **Declaration of Competing Interest**

508 The authors declare that they have no known competing financial interests or personal  
509 relationships that could have appeared to influence the work reported in this paper.

510 **References**

- 511 Acosta-González, A., Marqués, S., 2016. Bacterial diversity in oil-polluted marine coastal  
512 sediments. *Current Opinion in Biotechnology* 38, 24–32.  
513 <https://doi.org/10.1016/j.copbio.2015.12.010>
- 514 Amend, A., Burgaud, G., Cunliffe, M., Edgcomb, V.P., Ettinger, C.L., Gutiérrez, M.H.,  
515 Heitman, J., Hom, E.F.Y., Ianiri, G., Jones, A.C., Kagami, M., Picard, K.T., Quandt,  
516 C.A., Raghukumar, S., Riquelme, M., Stajich, J., Vargas-Muñiz, J., Walker, A.K.,  
517 Yarden, O., Gladfelter, A.S., 2019. Fungi in the Marine Environment: Open Questions  
518 and Unsolved Problems. *mBio* 10. <https://doi.org/10.1128/mBio.01189-18>
- 519 Bahram, M., Hildebrand, F., Forslund, S.K., Anderson, J.L., Soudzilovskaia, N.A., Bodegom,  
520 P.M., Bengtsson-Palme, J., Anslan, S., Coelho, L.P., Harend, H., Huerta-Cepas, J.,  
521 Medema, M.H., Maltz, M.R., Mundra, S., Olsson, P.A., Pent, M., Pölme, S., Sunagawa,  
522 S., Ryberg, M., Tedersoo, L., Bork, P., 2018. Structure and function of the global topsoil  
523 microbiome. *Nature* 560, 233–237. <https://doi.org/10.1038/s41586-018-0386-6>
- 524 Bandelj, V., Solidoro, C., Curiel, D., Cossarini, G., Melaku Canu, D., Rismondo, A., 2012.  
525 Fuzziness and Heterogeneity of Benthic Metacommunities in a Complex Transitional  
526 System. *PLOS ONE* 7, e52395. <https://doi.org/10.1371/journal.pone.0052395>
- 527 Ben Said, O., Louati, H., Soltani, A., Preud'homme, H., Cravo-Laureau, C., Got, P., Pringault,  
528 O., Aissa, P., Duran, R., 2015. Changes of benthic bacteria and meiofauna assemblages  
529 during bio-treatments of anthracene-contaminated sediments from Bizerta lagoon  
530 (Tunisia). *Environmental Science and Pollution Research* 22, 15319–15331.  
531 <https://doi.org/10.1007/s11356-015-4105-7>
- 532 Ben Salem, F., Ben Said, O., Cravo-Laureau, C., Mahmoudi, E., Bru, N., Monperrus, M.,  
533 Duran, R., 2019. Bacterial community assemblages in sediments under high  
534 anthropogenic pressure at Ichkeul Lake/Bizerte Lagoon hydrological system, Tunisia.  
535 *Environmental Pollution* 252, 644–656. <https://doi.org/10.1016/j.envpol.2019.05.146>
- 536 Board, T.E., 2015. Terrimonas, in: *Bergey's Manual of Systematics of Archaea and Bacteria*.  
537 American Cancer Society, pp. 1–3. <https://doi.org/10.1002/9781118960608.gbm00355>
- 538 Bolyen, E., Rideout, J.R., Dillon, M.R., Bokulich, N.A., Abnet, C.C., Al-Ghalith, G.A.,  
539 Alexander, H., Alm, E.J., Arumugam, M., Asnicar, F., Bai, Y., Bisanz, J.E., Bittinger,  
540 K., Brejnrod, A., Brislawn, C.J., Brown, C.T., Callahan, B.J., Caraballo-Rodríguez,  
541 A.M., Chase, J., Cope, E.K., Da Silva, R., Diener, C., Dorrestein, P.C., Douglas, G.M.,  
542 Durall, D.M., Duvallet, C., Edwardson, C.F., Ernst, M., Estaki, M., Fouquier, J.,  
543 Gauglitz, J.M., Gibbons, S.M., Gibson, D.L., Gonzalez, A., Gorlick, K., Guo, J.,  
544 Hillmann, B., Holmes, S., Holste, H., Huttenhower, C., Huttley, G.A., Janssen, S.,  
545 Jarmusch, A.K., Jiang, L., Kaehler, B.D., Kang, K.B., Keefe, C.R., Keim, P., Kelley,  
546 S.T., Knights, D., Koester, I., Kosciulek, T., Kreps, J., Langille, M.G.I., Lee, J., Ley,  
547 R., Liu, Y.-X., Loftfield, E., Lozupone, C., Maher, M., Marotz, C., Martin, B.D.,  
548 McDonald, D., McIver, L.J., Melnik, A.V., Metcalf, J.L., Morgan, S.C., Morton, J.T.,



549 Naimey, A.T., Navas-Molina, J.A., Nothias, L.F., Orchanian, S.B., Pearson, T., Peoples,  
550 S.L., Petras, D., Preuss, M.L., Pruesse, E., Rasmussen, L.B., Rivers, A., Robeson, M.S.,  
551 Rosenthal, P., Segata, N., Shaffer, M., Shiffer, A., Sinha, R., Song, S.J., Spear, J.R.,  
552 Swafford, A.D., Thompson, L.R., Torres, P.J., Trinh, P., Tripathi, A., Turnbaugh, P.J.,  
553 Ul-Hasan, S., van der Hooft, J.J.J., Vargas, F., Vázquez-Baeza, Y., Vogtman, E., von  
554 Hippel, M., Walters, W., Wan, Y., Wang, M., Warren, J., Weber, K.C., Williamson,  
555 C.H.D., Willis, A.D., Xu, Z.Z., Zaneveld, J.R., Zhang, Y., Zhu, Q., Knight, R.,  
556 Caporaso, J.G., 2019. Reproducible, interactive, scalable and extensible microbiome  
557 data science using QIIME 2. *Nature Biotechnology* 37, 852–857.  
558 <https://doi.org/10.1038/s41587-019-0209-9>

559 Bordenave, S., Fourçans, A., Blanchard, S., Goñi, M.S., Caumette, P., Duran, R., 2004.  
560 Structure and functional analyses of bacterial communities changes in microbial mats  
561 following petroleum exposure. *Ophelia* 58, 195–203.  
562 <https://doi.org/10.1080/00785236.2004.10410227>

563 Bourceret, A., Leyval, C., De Fouquet, C., Cébron, A., 2015. Mapping the centimeter-scale  
564 spatial variability of PAHs and microbial populations in the rhizosphere of two plants.  
565 *PLoS ONE* 10, 1–22. <https://doi.org/10.1371/journal.pone.0142851>

566 Bourceret, A., Leyval, C., Thomas, F., Cébron, A., 2017. Rhizosphere effect is stronger than  
567 PAH concentration on shaping spatial bacterial assemblages along centimetre-scale  
568 depth gradients. *Can. J. Microbiol.* 63, 881–893. <https://doi.org/10.1139/cjm-2017-0124>

570 Brannock, P.M., Ortmann, A.C., Moss, A.G., Halanych, K.M., 2016. Metabarcoding reveals  
571 environmental factors influencing spatio-temporal variation in pelagic micro-  
572 eukaryotes. *Molecular Ecology* 25, 3593–3604. <https://doi.org/10.1111/mec.13709>

573 Brown, J.H., 1984. On the Relationship between Abundance and Distribution of Species. *The*  
574 *American Naturalist* 124, 255–279. <https://doi.org/10.1086/284267>

575 Caceres, M.D., Legendre, P., 2009. Associations between species and groups of sites: indices  
576 and statistical inference, *Ecology*.

577 Callahan, B.J., McMurdie, P.J., Holmes, S.P., 2017. Exact sequence variants should replace  
578 operational taxonomic units in marker-gene data analysis. *ISME J* 11, 2639–2643.  
579 <https://doi.org/10.1038/ismej.2017.119>

580 Callahan, B.J., McMurdie, P.J., Rosen, M.J., Han, A.W., Johnson, A.J.A., Holmes, S.P., 2016.  
581 DADA2: High-resolution sample inference from Illumina amplicon data. *Nature*  
582 *Methods* 13, 581–583. <https://doi.org/10.1038/nmeth.3869>

583 Campbell, B.J., Kirchman, D.L., 2013. Bacterial diversity, community structure and potential  
584 growth rates along an estuarine salinity gradient. *ISME J* 7, 210–220.  
585 <https://doi.org/10.1038/ismej.2012.93>

586 Cardoso, P., Rigal, F., Carvalho, J.C., 2015. BAT - Biodiversity Assessment Tools, an R  
587 package for the measurement and estimation of alpha and beta taxon, phylogenetic and  
588 functional diversity. *Methods in Ecology and Evolution* 6, 232–236.  
589 <https://doi.org/10.1111/2041-210X.12310>

590 Cébron, A., Louvel, B., Faure, P., France-lanord, C., Chen, Y., Murrell, J.C., Leyval, C., 2011.  
591 Root exudates modify bacterial diversity of phenanthrene degraders in PAH-polluted  
592 soil but not phenanthrene degradation rates 13, 722–736.  
593 <https://doi.org/10.1111/j.1462-2920.2010.02376.x>

594 Chemidlin Prévost-Bouré, N., Christen, R., Dequiedt, S., Mougél, C., Lelièvre, M., Jolivet, C.,  
595 Shahbazkia, H.R., Guillou, L., Arrouays, D., Ranjard, L., 2011. Validation and  
596 Application of a PCR Primer Set to Quantify Fungal Communities in the Soil  
597 Environment by Real-Time Quantitative PCR. *PLoS One* 6, e24166.  
598 <https://doi.org/10.1371/journal.pone.0024166>

599 Chronopoulou, P.-M., Fahy, A., Coulon, F., Païssé, S., Goñi-Urriza, M., Peperzak, L., Acuña  
600 Alvarez, L., McKew, B.A., Lawson, T., Timmis, K.N., Duran, R., Underwood, G.J.C.,  
601 McGenity, T.J., 2013. Impact of a simulated oil spill on benthic phototrophs and  
602 nitrogen-fixing bacteria in mudflat mesocosms. *Environmental Microbiology* 15, 242–  
603 252. <https://doi.org/10.1111/j.1462-2920.2012.02864.x>

604 Comeau, A.M., Vincent, W.F., Bernier, L., Lovejoy, C., 2016. Novel chytrid lineages dominate  
605 fungal sequences in diverse marine and freshwater habitats. *Scientific Reports* 6, 30120.  
606 <https://doi.org/10.1038/srep30120>

607 Cravo-Laureau, C., Duran, R., 2014. Marine coastal sediments microbial hydrocarbon  
608 degradation processes: contribution of experimental ecology in the omics'era. *Frontiers*  
609 *in Microbiology* 5, 39. <https://doi.org/10.3389/fmicb.2014.00039>

610 Crump, B.C., Armbrust, E.V., Baross, J.A., 1999. Phylogenetic analysis of particle-attached  
611 and free-living bacterial communities in the Columbia river, its estuary, and the adjacent  
612 coastal ocean. *Appl Environ Microbiol* 65, 3192–3204.  
613 <https://doi.org/10.1128/AEM.65.7.3192-3204.1999>

614 Crump, B.C., Hopkinson, C.S., Sogin, M.L., Hobbie, J.E., 2004. Microbial biogeography along  
615 an estuarine salinity gradient: combined influences of bacterial growth and residence  
616 time. *Appl Environ Microbiol* 70, 1494–1505. [https://doi.org/10.1128/AEM.70.3.1494-  
617 1505.2004](https://doi.org/10.1128/AEM.70.3.1494-1505.2004)

618 Dufrêne, M., Legendre, P., 1997. Species assemblages and indicator species: the need for a  
619 flexible asymmetrical approach. *Ecological Monographs* 345–366.  
620 [https://doi.org/10.1890/0012-  
621 9615\(1997\)067\[0345:SAAST\]2.0.CO;2@10.1002/\(ISSN\)1557-  
622 7015\(CAT\)VirtualIssue\(VI\)ECM](https://doi.org/10.1890/0012-9615(1997)067[0345:SAAST]2.0.CO;2@10.1002/(ISSN)1557-7015(CAT)VirtualIssue(VI)ECM)

623 Duran, R., Bonin, P., Jezequel, R., Dubosc, K., Gassie, C., Terrisse, F., Abella, J., Cagnon, C.,  
624 Militon, C., Michotey, V., Gilbert, F., Cuny, P., Cravo-laureau, C., 2015a. Effect of  
625 physical sediments reworking on hydrocarbon degradation and bacterial community  
626 structure in marine coastal sediments. <https://doi.org/10.1007/s11356-015-4373-2>

627 Duran, R., Bonin, P., Jezequel, R., Dubosc, K., Gassie, C., Terrisse, F., Abella, J., Cagnon, C.,  
628 Militon, C., Michotey, V., Gilbert, F., Cuny, P., Cravo-Laureau, C., 2015b. Effect of  
629 physical sediments reworking on hydrocarbon degradation and bacterial community  
630 structure in marine coastal sediments. *Environmental Science and Pollution Research*  
631 22, 15248–15259. <https://doi.org/10.1007/s11356-015-4373-2>

632 Duran, R., Cravo-Laureau, C., 2016. Role of environmental factors and microorganisms in  
633 determining the fate of polycyclic aromatic hydrocarbons in the marine environment 1–  
634 17. <https://doi.org/10.1093/femsre/fuw031>

635 Engleberg, N.C., 2009. *Legionella*, *Bartonella*, *Haemophilus*, in: Schaechter, M. (Ed.),  
636 *Encyclopedia of Microbiology* (Third Edition). Academic Press, Oxford, pp. 170–181.  
637 <https://doi.org/10.1016/B978-012373944-5.00194-2>

- 638 Falkowski, P.G., Fenchel, T., Delong, E.F., 2008. The Microbial Engines That Drive Earth's  
639 Biogeochemical Cycles. *Science*. <https://doi.org/10.1126/science.1153213>
- 640 Finn, D.R., Yu, J., Ilhan, Z.E., Fernandes, V.M.C., Penton, C.R., Krajmalnik-Brown, R.,  
641 Garcia-Pichel, F., Vogel, T.M., 2020. MicroNiche: an R package for assessing microbial  
642 niche breadth and overlap from amplicon sequencing data. *FEMS Microbiology  
643 Ecology* 96, fiae131. <https://doi.org/10.1093/femsec/fiae131>
- 644 Fortunato, C.S., Crump, B.C., 2015. Microbial Gene Abundance and Expression Patterns across  
645 a River to Ocean Salinity Gradient. *PLOS ONE* 10, e0140578.  
646 <https://doi.org/10.1371/journal.pone.0140578>
- 647 Fredston-Hermann, A., Brown, C.J., Albert, S., Klein, C.J., Mangubhai, S., Nelson, J.L.,  
648 Teneva, L., Wenger, A., Gaines, S.D., Halpern, B.S., 2016. Where Does River Runoff  
649 Matter for Coastal Marine Conservation? *Frontiers in Marine Science* 3.  
650 <https://doi.org/10.3389/fmars.2016.00273>
- 651 Graham, E.B., Knelman, J.E., Schindlbacher, A., Siciliano, S., Breulmann, M., Yannarell, A.,  
652 Beman, J.M., Abell, G., Philippot, L., Prosser, J., Foulquier, A., Yuste, J.C., Glanville,  
653 H.C., Jones, D.L., Angel, R., Salminen, J., Newton, R.J., Bürgmann, H., Ingram, L.J.,  
654 Hamer, U., Siljanen, H.M.P., Peltoniemi, K., Potthast, K., Bañeras, L., Hartmann, M.,  
655 Banerjee, S., Yu, R.-Q., Nogaro, G., Richter, A., Koranda, M., Castle, S.C., Goberna,  
656 M., Song, B., Chatterjee, A., Nunes, O.C., Lopes, A.R., Cao, Y., Kaisermann, A., Hallin,  
657 S., Strickland, M.S., Garcia-Pausas, J., Barba, J., Kang, H., Isobe, K., Papaspyrou, S.,  
658 Pastorelli, R., Lagomarsino, A., Lindström, E.S., Basiliko, N., Nemergut, D.R., 2016.  
659 Microbes as Engines of Ecosystem Function: When Does Community Structure  
660 Enhance Predictions of Ecosystem Processes? *Frontiers in Microbiology* 7.
- 661 Grizzetti, B., Liqueste, C., Pistocchi, A., Vigiak, O., Zulian, G., Bouraoui, F., Roo, A.D.,  
662 Cardoso, A.C., 2019. Relationship between ecological condition and ecosystem services  
663 in European rivers, lakes and coastal waters. *Science of The Total Environment* 671,  
664 452–465. <https://doi.org/10.1016/j.scitotenv.2019.03.155>
- 665 Gu, H., Lou, J., Wang, H., Yang, Y., Wu, L., Wu, J., Xu, J., 2016. Biodegradation, Biosorption  
666 of Phenanthrene and Its Trans-Membrane Transport by *Massilia* sp. WF1 and  
667 *Phanerochaete chrysosporium*. *Front. Microbiol.* 7.  
668 <https://doi.org/10.3389/fmicb.2016.00038>
- 669 Halliday, E., McLellan, S.L., Amaral-Zettler, L.A., Sogin, M.L., Gast, R.J., 2014. Comparison  
670 of Bacterial Communities in Sands and Water at Beaches with Bacterial Water Quality  
671 Violations. *PLoS ONE* 9, e90815. <https://doi.org/10.1371/journal.pone.0090815>
- 672 Hanski, I., 1982. Dynamics of Regional Distribution: The Core and Satellite Species  
673 Hypothesis. *Oikos* 38, 210–221. <https://doi.org/10.2307/3544021>
- 674 Heberle, H., Meirelles, G.V., da Silva, F.R., Telles, G.P., Minghim, R., 2015. InteractiVenn: a  
675 web-based tool for the analysis of sets through Venn diagrams. *BMC Bioinformatics*  
676 16, 169. <https://doi.org/10.1186/s12859-015-0611-3>
- 677 Hoffman, E.J., Mills, G.L., Latimer, J.S., Quinn, J.G., 1984. Urban runoff as a source of  
678 polycyclic aromatic hydrocarbons to coastal waters. *Environmental Science &  
679 Technology* 18, 580–587. <https://doi.org/10.1021/es00126a003>
- 680 Holmsgaard, P.N., Norman, A., Hede, S.Chr., Poulsen, P.H.B., Al-Soud, W.A., Hansen, L.H.,  
681 Sørensen, S.J., 2011. Bias in bacterial diversity as a result of Nycodenz extraction from

- 682 bulk soil. *Soil Biology and Biochemistry* 43, 2152–2159.  
683 <https://doi.org/10.1016/j.soilbio.2011.06.019>
- 684 Hu, A., Wang, H., Yang, X., Hou, L., Li, J., Li, S., Yu, C.-P., 2017. Seasonal and spatial  
685 variations of prokaryoplankton communities in a salinity-influenced watershed, China.  
686 *FEMS Microbiology Ecology* 93. <https://doi.org/10.1093/femsec/fix093>
- 687 Jeanbille, M., Gury, J., Duran, R., Tronczynski, J., Agogué, H., Ben Saïd, O., Ghiglione, J.-F.,  
688 Auguet, J.-C., 2016. Response of Core Microbial Consortia to Chronic Hydrocarbon  
689 Contaminations in Coastal Sediment Habitats. *Front. Microbiol.* 7.  
690 <https://doi.org/10.3389/fmicb.2016.01637>
- 691 Jeffries, T.C., Schmitz Fontes, M.L., Harrison, D.P., Van-Dongen-Vogels, V., Eyre, B.D.,  
692 Ralph, P.J., Seymour, J.R., 2016. Bacterioplankton dynamics within a large  
693 anthropogenically impacted urban estuary. *Frontiers in Microbiology*.  
694 <https://doi.org/10.3389/fmicb.2015.01438>
- 695 Jones, E.B.G., Suetrong, S., Sakayaroj, J., Bahkali, A.H., Abdel-Wahab, M.A., Boekhout, T.,  
696 Pang, K.-L., 2015. Classification of marine Ascomycota, Basidiomycota,  
697 Blastocladiomycota and Chytridiomycota. *Fungal Diversity* 73, 1–72.  
698 <https://doi.org/10.1007/s13225-015-0339-4>
- 699 Jurburg, S.D., Nunes, I., Brejnrod, A., Jacquioud, S., Priemé, A., Sørensen, S.J., Van Elsas, J.D.,  
700 Salles, J.F., 2017. Legacy Effects on the Recovery of Soil Bacterial Communities from  
701 Extreme Temperature Perturbation. *Front Microbiol* 8, 1832.  
702 <https://doi.org/10.3389/fmicb.2017.01832>
- 703 Knights, D., Kuczynski, J., Charlson, E.S., Zaneveld, J., Mozer, M.C., Collman, R.G.,  
704 Bushman, F.D., Knight, R., Kelley, S.T., 2011. Bayesian community-wide culture-  
705 independent microbial source tracking. *Nature Methods* 8, 761–763.  
706 <https://doi.org/10.1038/nmeth.1650>
- 707 Kohlmeyer, J., Kohlmeyer, E., 1979. *Marine mycology, the higher fungi*: Academic Press, in:  
708 New York. San Fransisco.
- 709 Levins, R., 1968. *Evolution in Changing Environments*. Princeton University Press, Princeton,  
710 NJ, USA.
- 711 Lindh, M.V., Sjöstedt, J., Ekstam, B., Casini, M., Lundin, D., Hugerth, L.W., Hu, Y.O.O.,  
712 Andersson, A.F., Andersson, A., Legrand, C., Pinhassi, J., 2017. Metapopulation theory  
713 identifies biogeographical patterns among core and satellite marine bacteria scaling  
714 from tens to thousands of kilometers. *Environ Microbiol* 19, 1222–1236.  
715 <https://doi.org/10.1111/1462-2920.13650>
- 716 Logares, R., Bråte, J., Bertilsson, S., Clasen, J.L., Shalchian-Tabrizi, K., Rengefors, K., 2009.  
717 Infrequent marine-freshwater transitions in the microbial world. *Trends Microbiol* 17,  
718 414–422. <https://doi.org/10.1016/j.tim.2009.05.010>
- 719 Louca, S., Parfrey, L.W., Doebeli, M., 2016. Decoupling function and taxonomy in the global  
720 ocean microbiome. *Science* 353, 1272–1277. <https://doi.org/10.1126/science.aaf4507>
- 721 Lozupone, C., Knight, R., 2005. UniFrac: a New Phylogenetic Method for Comparing  
722 Microbial Communities. *Applied and Environmental Microbiology* 71, 8228–8235.  
723 <https://doi.org/10.1128/AEM.71.12.8228-8235.2005>
- 724 Lozupone, C.A., Knight, R., 2007. Global patterns in bacterial diversity. *Proceedings of the*  
725 *National Academy of Sciences* 104, 11436–11440.

- 726 Magurran, A.E., Henderson, P.A., 2003. Explaining the excess of rare species in natural species  
727 abundance distributions. *Nature* 422, 714–716. <https://doi.org/10.1038/nature01547>
- 728 Mansour, I., Heppell, C.M., Ryo, M., Rillig, M.C., 2018. Application of the microbial  
729 community coalescence concept to riverine networks. *Biological Reviews* 93, 1832–  
730 1845. <https://doi.org/10.1111/brv.12422>
- 731 McGenity, T.J., Folwell, B.D., McKew, B.A., Sanni, G.O., 2012. Marine crude-oil  
732 biodegradation: a central role for interspecies interactions. *Aquat Biosyst* 8, 10.  
733 <https://doi.org/10.1186/2046-9063-8-10>
- 734 McMurdie, P.J., Holmes, S., 2013. phyloseq: An R package for reproducible interactive  
735 analysis and graphics of microbiome census data. *PLoS ONE* 8, e61217.
- 736 Money, N.P., 2016. Chapter 3 - Spore Production, Discharge, and Dispersal, in: Watkinson,  
737 S.C., Boddy, L., Money, N.P. (Eds.), *The Fungi* (Third Edition). Academic Press,  
738 Boston, pp. 67–97. <https://doi.org/10.1016/B978-0-12-382034-1.00003-7>
- 739 Montgomery, D.R., Zabowski, D., Ugolini, F.C., Hallberg, R.O., Spaltenstein, H., 2000. 8 -  
740 Soils, Watershed Processes, and Marine Sediments, in: Jacobson, M.C., Charlson, R.J.,  
741 Rodhe, H., Orians, G.H. (Eds.), *International Geophysics, Earth System Science*.  
742 Academic Press, pp. 159–iv. [https://doi.org/10.1016/S0074-6142\(00\)80114-X](https://doi.org/10.1016/S0074-6142(00)80114-X)
- 743 Nagase, A., Dunnett, N., 2012. Amount of water runoff from different vegetation types on  
744 extensive green roofs: Effects of plant species, diversity and plant structure. *Landscape*  
745 *and Urban Planning* 104, 356–363. <https://doi.org/10.1016/j.landurbplan.2011.11.001>
- 746 Nelson, M.B., Martiny, A.C., Martiny, J.B.H., 2016. Global biogeography of microbial  
747 nitrogen-cycling traits in soil. *PNAS* 113, 8033–8040.  
748 <https://doi.org/10.1073/pnas.1601070113>
- 749 Nguyen, N.H., Song, Z., Bates, S.T., Branco, S., Tedersoo, L., Menke, J., Schilling, J.S.,  
750 Kennedy, P.G., 2016. FUNGuild: An open annotation tool for parsing fungal  
751 community datasets by ecological guild. *Fungal Ecology* 20, 241–248.  
752 <https://doi.org/10.1016/j.funeco.2015.06.006>
- 753 Nunes, I., Jurburg, S., Jacquiod, S., Brejnrod, A., Falcão Salles, J., Priemé, A., Sørensen, S.J.,  
754 2018. Soil bacteria show different tolerance ranges to an unprecedented disturbance.  
755 *Biology and Fertility of Soils* 54, 189–202. <https://doi.org/10.1007/s00374-017-1255-4>
- 756 Ofek, M., Hadar, Y., Minz, D., 2012. Ecology of Root Colonizing Massilia (Oxalobacteraceae).  
757 *PLOS ONE* 7, 1–12. <https://doi.org/10.1371/journal.pone.0040117>
- 758 Oksanen, J., Blanchet, F.G., Kindt, R., Legendre, P., Minchin, P., O'Hara, R., Simpson, G.,  
759 Solymos, P., Stevens, M., Wagner, H., 2013. *Vegan: Community Ecology Package*. R  
760 Package Version. 2.0-10. CRAN.
- 761 Paissé, S., Coulon, F., Goñi-Urriza, M., Peperzak, L., McGenity, T.J., Duran, R., 2008.  
762 Structure of bacterial communities along a hydrocarbon contamination gradient in a  
763 coastal sediment. *FEMS Microbiology Ecology* 66, 295–305.  
764 <https://doi.org/10.1111/j.1574-6941.2008.00589.x>
- 765 Pang, K.-L., Guo, S.-Y., Chen, I.-A., Burgaud, G., Luo, Z.-H., Dahms, H.U., Hwang, J.-S., Lin,  
766 Y.-L., Huang, J.-S., Ho, T.-W., Tsang, L.-M., Chiang, M.W.-L., Cha, H.-J., 2019.  
767 Insights into fungal diversity of a shallow-water hydrothermal vent field at Kueishan  
768 Island, Taiwan by culture-based and metabarcoding analyses. *PLOS ONE* 14,  
769 e0226616. <https://doi.org/10.1371/journal.pone.0226616>

770 Parada, A.E., Needham, D.M., Fuhrman, J.A., 2016. Every base matters: assessing small  
771 subunit rRNA primers for marine microbiomes with mock communities, time series and  
772 global field samples. *Environmental Microbiology* 18, 1403–1414.  
773 <https://doi.org/10.1111/1462-2920.13023>

774 Paradis, E., Schliep, K., 2019. ape 5.0: an environment for modern phylogenetics and  
775 evolutionary analyses in R. *Bioinformatics* 35, 526–528.  
776 <https://doi.org/10.1093/bioinformatics/bty633>

777 Pathom-Aree, W., Nogi, Y., Sutcliffe, I.C., Ward, A.C., Horikoshi, K., Bull, A.T., Goodfellow,  
778 M., 2006. *Williamsia marianensis* sp. nov., a novel actinomycete isolated from the  
779 Mariana Trench. *International Journal of Systematic and Evolutionary Microbiology*  
780 56, 1123–1126. <https://doi.org/10.1099/ijs.0.64132-0>

781 Paver, S.F., Muratore, D., Newton, R.J., Coleman, M.L., 2018. Reevaluating the Salty Divide:  
782 Phylogenetic Specificity of Transitions between Marine and Freshwater Systems.  
783 *mSystems* 3. <https://doi.org/10.1128/mSystems.00232-18>

784 Pischedda, L., Poggiale, J.C., Cuny, P., Gilbert, F., 2008. Imaging Oxygen Distribution in  
785 Marine Sediments. The Importance of Bioturbation and Sediment Heterogeneity. *Acta*  
786 *Biotheor* 56, 123–135. <https://doi.org/10.1007/s10441-008-9033-1>

787 Price, M.N., Arkin, A.P., Dehal, P.S., 2010. Fasttree 2—approximately maximum-likelihood  
788 trees for large alignments. *PloS one*.

789 Quast, C., Pruesse, E., Yilmaz, P., Gerken, J., Schweer, T., Yarza, P., Peplies, J., Glöckner,  
790 F.O., 2013. The SILVA ribosomal RNA gene database project: improved data  
791 processing and web-based tools. *Nucleic Acids Research* 41, D590–D596.  
792 <https://doi.org/10.1093/nar/gks1219>

793 R Core Team, 2021. R: A Language and Environment for Statistical Computing. R Foundation  
794 for Statistical Computing, Vienna, Austria.

795 Rillig, M.C., Antonovics, J., Caruso, T., Lehmann, A., Powell, J.R., Veresoglou, S.D.,  
796 Verbruggen, E., 2015. Interchange of entire communities: microbial community  
797 coalescence. *Trends in Ecology & Evolution* 30, 470–476.  
798 <https://doi.org/10.1016/j.tree.2015.06.004>

799 Rocca, J.D., Simonin, M., Bernhardt, E.S., Washburne, A.D., Wright, J.P., 2020. Rare microbial  
800 taxa emerge when communities collide: freshwater and marine microbiome responses  
801 to experimental mixing. *Ecology* 101. <https://doi.org/10.1002/ecy.2956>

802 Rojas-Jimenez, K., Wurzbacher, C., Bourne, E.C., Chiuchiolo, A., Priscu, J.C., Grossart, H.-P.,  
803 2017. Early diverging lineages within Cryptomycota and Chytridiomycota dominate the  
804 fungal communities in ice-covered lakes of the McMurdo Dry Valleys, Antarctica.  
805 *Scientific Reports* 7, 15348. <https://doi.org/10.1038/s41598-017-15598-w>

806 Stach, J.E.M., Maldonado, L.A., Ward, A.C., Bull, A.T., Goodfellow, M., 2004. *Williamsia*  
807 *maris* sp. nov., a novel actinomycete isolated from the Sea of Japan. *International*  
808 *Journal of Systematic and Evolutionary Microbiology* 54, 191–194.  
809 <https://doi.org/10.1099/ijs.0.02767-0>

810 Stauffert, M., Cravo-laureau, C., Duran, R., 2015. Dynamic of sulphate-reducing  
811 microorganisms in petroleum-contaminated marine sediments inhabited by the  
812 polychaete *Hediste diversicolor* 15273–15284. [https://doi.org/10.1007/s11356-014-](https://doi.org/10.1007/s11356-014-3624-y)  
813 [3624-y](https://doi.org/10.1007/s11356-014-3624-y)

- 814 Stauffert, M., Duran, R., Gassie, C., 2014. Response of Archaeal Communities to Oil Spill in  
815 Bioturbated Mudflat Sediments 108–119. <https://doi.org/10.1007/s00248-013-0288-y>
- 816 Tolosa, I., de Mora, S., Sheikholeslami, M.R., Villeneuve, J.-P., Bartocci, J., Cattini, C., 2004.  
817 Aliphatic and aromatic hydrocarbons in coastal caspian Sea sediments. *Marine Pollution*  
818 *Bulletin* 48, 44–60. [https://doi.org/10.1016/S0025-326X\(03\)00255-8](https://doi.org/10.1016/S0025-326X(03)00255-8)
- 819 Torres, M.S., White, J.F., 2009. Clavicipitaceae: Free-Living and Saprotrophs to Plant  
820 Endophytes, in: Schaechter, M. (Ed.), *Encyclopedia of Microbiology* (Third Edition).  
821 Academic Press, Oxford, pp. 422–430. [https://doi.org/10.1016/B978-012373944-](https://doi.org/10.1016/B978-012373944-5.00329-1)  
822 [5.00329-1](https://doi.org/10.1016/B978-012373944-5.00329-1)
- 823 Toyama, T., Furukawa, T., Maeda, N., Inoue, D., Sei, K., Mori, K., Kikuchi, S., Ike, M., 2011.  
824 Accelerated biodegradation of pyrene and benzo[a]pyrene in the Phragmites australis  
825 rhizosphere by bacteria–root exudate interactions. *Water Research* 45, 1629–1638.  
826 <https://doi.org/10.1016/j.watres.2010.11.044>
- 827 Ulrich, W., Zalewski, M., 2006. Abundance and co-occurrence patterns of core and satellite  
828 species of ground beetles on small lake islands. *Oikos* 114, 338–348.  
829 <https://doi.org/10.1111/j.2006.0030-1299.14773.x>
- 830 Unterseher, M., Jumpponen, A., Öpik, M., Tedersoo, L., Moora, M., Dormann, C.F., Schnittler,  
831 M., 2011. Species abundance distributions and richness estimations in fungal  
832 metagenomics – lessons learned from community ecology. *Molecular Ecology* 20, 275–  
833 285. <https://doi.org/10.1111/j.1365-294X.2010.04948.x>
- 834 Vainio, E.J., Hantula, J., 2000. Direct analysis of wood-inhabiting fungi using denaturing  
835 gradient gel electrophoresis of amplified ribosomal DNA. *Mycological Research* 104,  
836 927–936. <https://doi.org/10.1017/S0953756200002471>
- 837 van der Gast, C.J., Walker, A.W., Stressmann, F.A., Rogers, G.B., Scott, P., Daniels, T.W.,  
838 Carroll, M.P., Parkhill, J., Bruce, K.D., 2011. Partitioning core and satellite taxa from  
839 within cystic fibrosis lung bacterial communities. *ISME J* 5, 780–791.  
840 <https://doi.org/10.1038/ismej.2010.175>
- 841 Van Hecke, M.M., Treonis, A.M., Kaufman, J.R., 2005. How does the Fungal Endophyte  
842 *Neotyphodium coenophialum* Affect Tall Fescue (*Festuca arundinacea*)  
843 Rhizodeposition and Soil Microorganisms? *Plant Soil* 275, 101–109.  
844 <https://doi.org/10.1007/s11104-005-0380-2>
- 845 Wang, Y., Qian, P.-Y., 2009. Conservative fragments in bacterial 16S rRNA genes and primer  
846 design for 16S ribosomal DNA amplicons in metagenomic studies. *PLoS ONE* 4, e7401.  
847 <https://doi.org/10.1371/journal.pone.0007401>
- 848 Webster, G., O’Sullivan, L.A., Meng, Y., Williams, A.S., Sass, A.M., Watkins, A.J., Parkes,  
849 R.J., Weightman, A.J., 2015. Archaeal community diversity and abundance changes  
850 along a natural salinity gradient in estuarine sediments. *FEMS Microbiol Ecol* 91, 1–  
851 18. <https://doi.org/10.1093/femsec/fiu025>
- 852 Wenzel, W.W., 2009. Rhizosphere processes and management in plant-assisted bioremediation  
853 (phytoremediation) of soils. *Plant Soil* 321, 385–408. [https://doi.org/10.1007/s11104-](https://doi.org/10.1007/s11104-008-9686-1)  
854 [008-9686-1](https://doi.org/10.1007/s11104-008-9686-1)
- 855 Wisnoski, N.I., Muscarella, M.E., Larsen, M.L., Peralta, A.L., Lennon, J.T., 2020. Metabolic  
856 insight into bacterial community assembly across ecosystem boundaries. *Ecology* 101,  
857 e02968. <https://doi.org/10.1002/ecy.2968>

- 858 Yakirevich, A., Pachepsky, Y.A., Guber, A.K., Gish, T.J., Shelton, D.R., Cho, K.H., 2013.  
859 Modeling transport of *Escherichia coli* in a creek during and after artificial high-flow  
860 events: three-year study and analysis. *Water Res.* 47, 2676–2688.  
861 <https://doi.org/10.1016/j.watres.2013.02.011>
- 862 Yassin, A.F., Young, C.C., Lai, W.-A., Hupfer, H., Arun, A.B., Shen, F.-T., Rekha, P.D., Ho,  
863 M.-J., 2007. *Williamsia serinedens* sp. nov., isolated from an oil-contaminated soil.  
864 *International Journal of Systematic and Evolutionary Microbiology* 57, 558–561.  
865 <https://doi.org/10.1099/ijs.0.64691-0>
- 866



867 **Table 1.** ASV indicators of coalescence identified by the indicator value index (IndVal). ASV  
868 indicators specifically associated to sediment with runoff (SedR tf) were identified by an  
869 indicator analysis performed among conditions in the sediment compartment. In a second step,  
870 the IndVal of each ASV indicator was calculated among soil, runoff and sediment  
871 compartments. IndVal value range from 0 (no association) to 1 (perfect association). Only  
872 ASVs indicators with significant IndVal index are presented (p for p-value).

Indicator analysis				Sediment compartment's conditions			Soil, runoff and sediment compartments		
ASV	Taxonomic affiliation			IndVal	p	association	IndVal	p	association
525	Fungi	Pezizomycotina	<i>Hypocreales</i>	0.850	0.015	SedR tf	0.779	0.005	Soil
2716	Bacteria	Alphaproteobacteria	<i>Rhodobacteraceae</i>	0.764	0.045	SedR tf	0.540	0.005	Sed
635	Bacteria	Deltaproteobacteria	NA	0.844	0.025	SedR tf	0.707	0.005	Sed
3543	Bacteria	Bacteroidia	<i>Cyclobacteriaceae</i>	0.857	0.01	SedR tf	0.707	0.005	Sed

873

874 **Figure 1.** Experimental design. Schema of the land-sea continuum microcosm (A) mimicking  
875 the terrigenous inputs to marine coastal sediment by soil runoff (left). Control microcosm (right)  
876 corresponds to sediment without soil runoff. Photo of the experiment (B). Schematic  
877 representation of the microcosms (C) with the different conditions applied to the soil and  
878 sediment compartments: Soil: soil; Runoff: runoff water (with terrigenous inputs); Sed:  
879 sediment; SedR: sediment receiving runoff; SedNR: Sed without runoff; NP: non-planted; P:  
880 planted; NC: without HC spiking; C: HC spiking. Each condition was performed in triplicate.

881

882 **Figure 2.** Microbial alpha-diversity in soil and in sediment. Taxonomic (left) and phylogenetic  
883 (right) alpha-diversity indices for the prokaryotic (A) and the fungal (B) communities in soil,  
884 and for the prokaryotic (C) and the fungal (D) communities in sediment, in the different  
885 experimental conditions. Error bars represent standard deviation of three replicates for each  
886 condition. Letters represent pairwise contrasts ( $p < 0.05$ ) of sample conditions. R: richness; <sup>2</sup>D:  
887 Inverse Simpson index; Faith's PD: Faith's phylogenetic diversity index; Hill <sup>2</sup>PD:  
888 phylogenetic diversity index based on Hill 2 number; Soil: soil; Sed: sediment; R: with runoff;  
889 NR: without runoff; NC: without HC spiking; C: with HC spiking; P: planted; NP: non-planted;  
890 t0: beginning of the experiment; tf: end of the experiment (after 39 days of incubation).

891

892 **Figure 3.** Composition of the prokaryotic (A) and the fungal (B) communities in soil, runoff  
893 water and sediment, in the different conditions (NC: without HC spiking; C: with HC spiking;  
894 NP: non-planted; P: planted; NR: without runoff; R: with runoff; t0: beginning of the  
895 experiment; t1 and t2: 16 and 30 days of incubation; tf: end of the experiment, after 39 days  
896 incubation). The analysis was performed at the phylum level with Proteobacteria split into  
897 classes. Phyla <1% abund.: phyla with total relative abundance less than 1% ranked by

898 decreasing relative abundance, including unassigned, Thaumarchaeota, Firmicutes,  
899 Fibrobacteres, Fusobacteria, Nitrospirae, Omninitrophaeota, Latescibacteria,  
900 Armatimonadetes, Patescibacteria, Spirochaetes, Calditrichaeota, Rokubacteria,  
901 Marinimicrobia (SAR406 clade), Tenericutes, Dadabacteria, Dependuntiae, Elusimicrobia,  
902 Zixibacteria, Nanoarchaeaeota, unassigned Proteobacteria, Epsilonproteobacteria, candidate  
903 phylum WPS-2 (or Eremiobacterota), Deinococcus-Thermus, Cloacimonetes, Abditibacteriota  
904 (previously known as FBP candidatus).

905

906 **Figure 4.** NMDS analysis based on the weighted UniFrac metrics presenting the differences  
907 observed in the prokaryotic (A) and in the fungal (B) community composition of soil, runoff  
908 and sediment compartments. Coloured segments connect samples with the same plant condition  
909 and sampling date to their average point while shapes indicate if samples were HC spiked  
910 (circle) or not (triangle). NR: without runoff (control); R: with runoff; NP: non-planted; P:  
911 planted; NC: without HC spiking; C: with HC spiking; t0: beginning of the experiment; t1: 16  
912 days of incubation; t2: 30 days of incubation; tf: end of the experiment.

913

914 **Figure 5.** Venn diagrams of prokaryotic (A) and fungal (B) core communities from the different  
915 compartments and the distribution of transferred prokaryotic (C) and fungal (D) ASVs in soil,  
916 runoff and sediment. Soil (t0&tf): ASVs present in soil at the beginning (t0) and at the end of  
917 the experiment (tf); Runoff (t1&t2): ASVs present in runoff after 16 (t1) and 30 (t2) days of  
918 incubation; Sed t0: ASVs in sediment at the beginning of the experiment (t0); SedR tf: ASVs  
919 in sediment with runoff at the end of the experiment (tf); SedNR tf, ASVs present in sediment  
920 without runoff at the end of the experiment (tf). The total number of ASVs in each compartment  
921 is indicated in parenthesis. The microbial ASVs exclusively shared between soil, runoff and  
922 sediment with runoff was coloured in red and were probably transferred from soil to sediment

923 by runoff. In C and D, the data represent the mean of three biological replicates ( $n = 3$ ). R:  
924 sediment with runoff; NR: sediment without runoff; NP: non-planted; P: planted; NC: without  
925 HC spiking; C: with HC spiking.

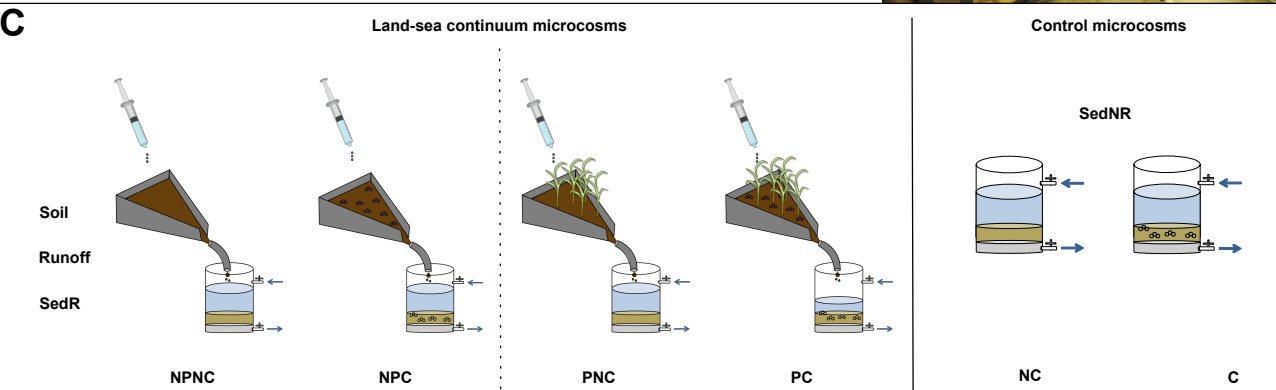
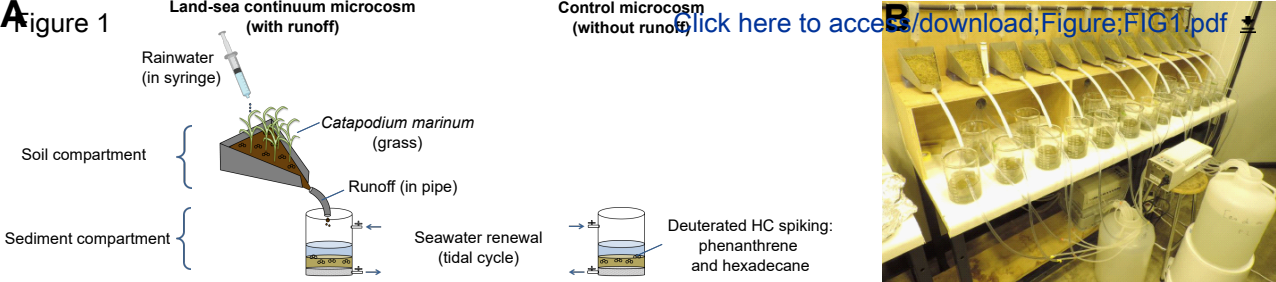
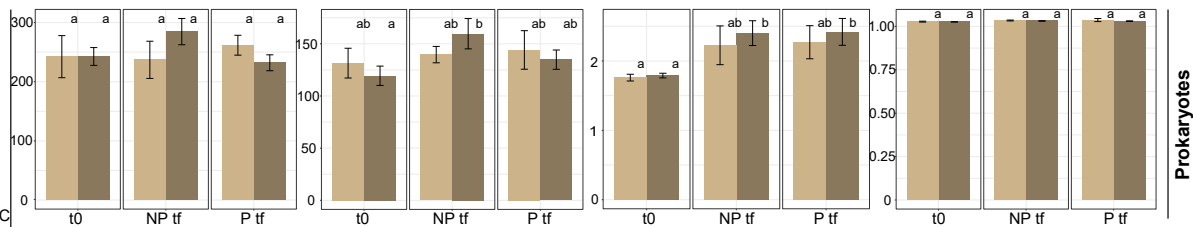


Figure 2

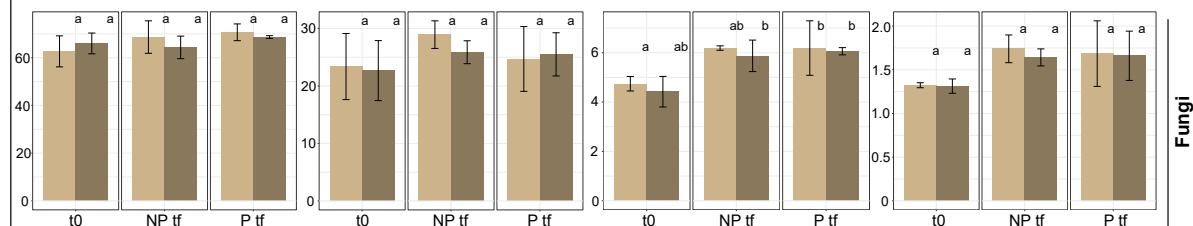
ASV alpha-diversity

Phylogenetic alpha-diversity  
Faith's PD

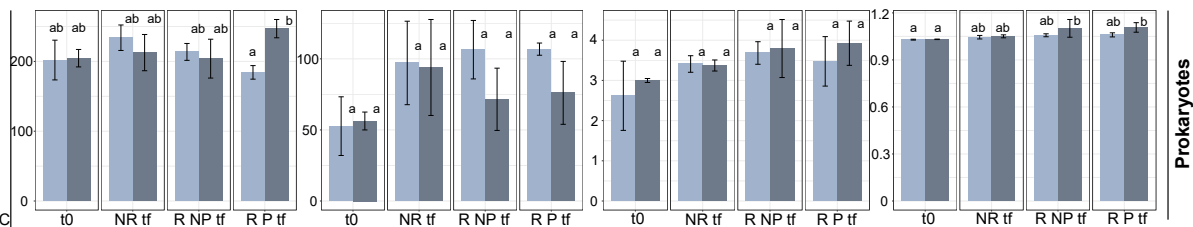
A



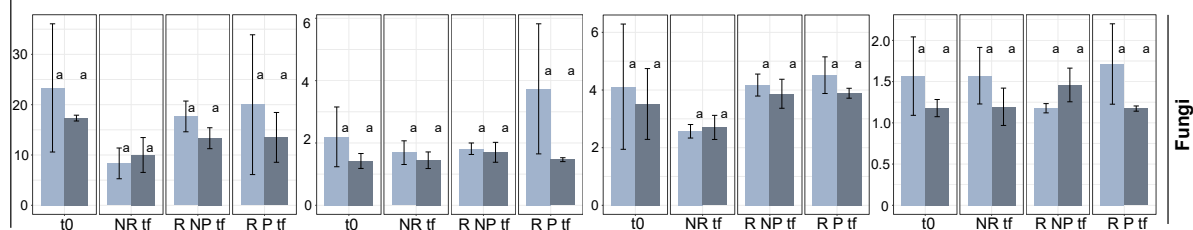
B

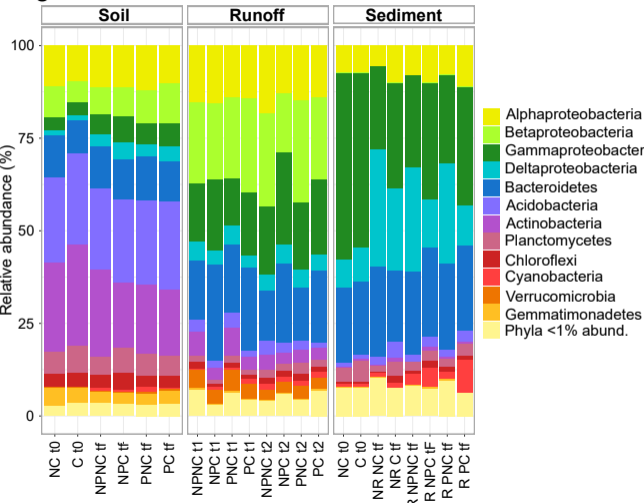
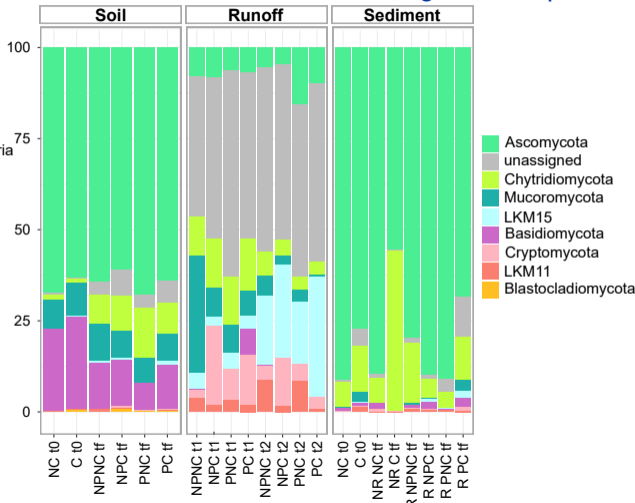


C

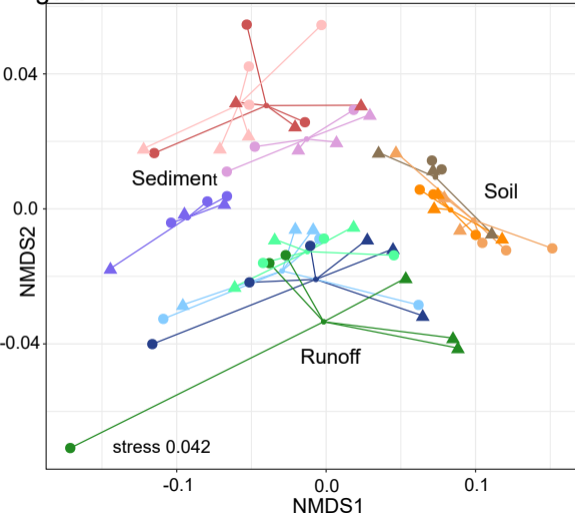


D

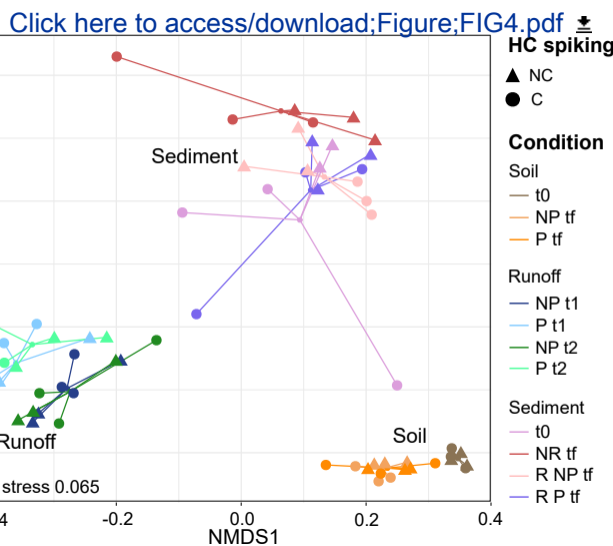


**A** Figure 3**B** [Click here to access/download;Figure;FIG3.pdf](#) 

**A** Figure 4

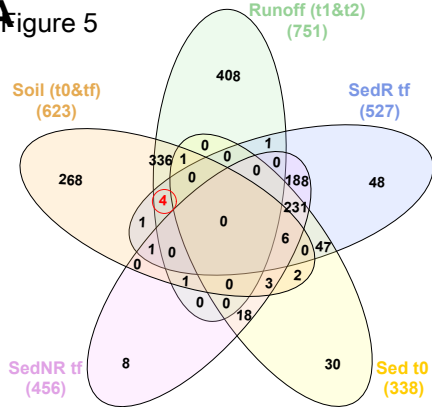


**B**

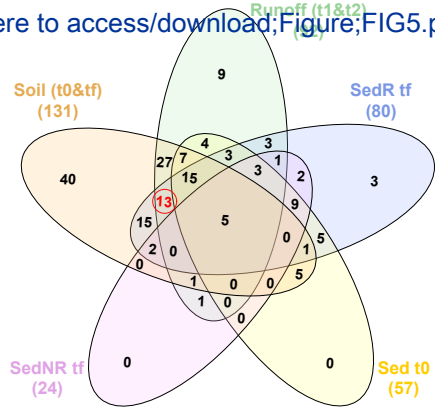




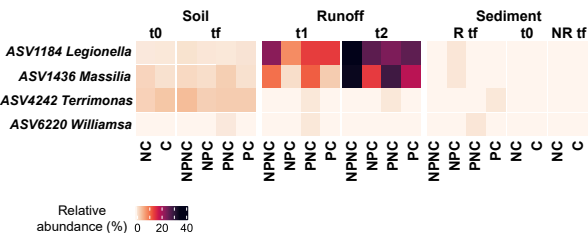
**A** Figure 5



**B** [Click here to access/download;Figure;FIG5.pdf](#)



**C**



**D**

